REFERENCES

[1] C. T. Chen, *Linear System Theory and Design.* New York: Holt, Rinehart and Winston, 1984.
[2] J. M. Maciejowski, *Multivariable Feedback Design.* New York: Addison-Wesley, 1989.
[3] M. Vidyasagar, "Optimal rejection of persistent bounded disturbances," *IEEE Trans. Automat. Contr.*, vol. AC-31, no. 6, pp. 527-534, June 1986.
[4] J. J. E. Slotine and W. Li, *Applied Nonlinear Control.* Englewood Cliffs, NJ: Prentice-Hall, 1991.
[5] J. C. Willems, "Dissipative dynamical systems," *Arch. Rational Mechanics Anal.*, vol. 45, pp. 321-393, 1972.
[6] J. S. Shamma and M. Athans, "Analysis of gain scheduled control for nonlinear plants," *IEEE Trans. Automat. Contr.*, vol. 34, no. 8, pp. 898-907, Aug. 1990.
[7] B. Kosko, *Neural Networks and Fuzzy Systems.* Englewood Cliffs, NJ: Prentice-Hall, 1992.
[8] M. F. Golnaraghi, "Regulation of flexible structures via nonlinear coupling," *J. Dynamics Contr.*, vol. 1, pp. 405-428, 1991.
[9] M. F. Golnaraghi, K. L. Tuer, and D. Wang, "Regulation of flexible structures via internal resonance using nonlinear enhancement," *J. Dynamics Contr.*, vol. 4, pp. 73-96, 1994.
[10] K. L. Tuer, A. P. Duquette, and M. F. Golnaraghi, "Vibration control of a flexible beam using a rotational internal resonance controller part I: Theoretical development and analysis," *J. Sound Vibration*, vol. 163, no. 3, 1993.
[11] A. P. Duquette, K. L. Tuer, and M. F. Golnaraghi, "Vibration control of a flexible beam using a rotational internal resonance controller part II: Experiment," *J. Sound Vibration*, vol. 163, no. 3, 1993.
[12] A. P. Duquette, "An experimental study of vibration control of a flexible beam via modal and coordinate coupling," Master's thesis, Univ. of Waterloo, Waterloo, Ontario, Canada, 1991.
[13] K. L. Tuer, "Vibration control of flexible structures using nonlinear and linear coupling effects," Master's thesis, Univ. of Waterloo, Waterloo, Ontario, Canada, 1991.
[14] K. L. Tuer, M. F. Golnaraghi, and D. Wang, "Development of a generalised active vibration suppression strategy for a cantilever beam using internal resonance," *J. Nonlinear Dynamics*, vol. 5, no. 2, pp. 131-151, 1994.
[15] K. L. Tuer, "Towards the formulation of generalised vibration suppression laws using linear and nonlinear coupling paradigms," Ph.D. dissertation, Dept. Elec. Comp. Eng., Univ. of Waterloo, Waterloo, Ontario, Canada, 1994.
[16] K. L. Tuer, M. F. Golnaraghi, and D. Wang, "Multi-mode vibration suppression of oscillatory systems via coupling effects," *IEEE Trans. Automat. Contr.*, submitted.
[17] A. H. Nayfeh and D. T. Mook, *Nonlinear Oscillations.* New York: Wiley, 1979.

μ-Synthesis of an Electromagnetic Suspension System

Masayuki Fujita, Toru Namerikawa,
Fumio Matsumura, and Kenko Uchida

***Abstract*— This paper deals with μ-synthesis of an electromagnetic suspension system. First, an issue of modeling a real physical electromagnetic suspension system is discussed. We derive a nominal model as well as a set of models in which the real system is assumed to reside. Different model structures and possible model parameter values are fully employed to determine unstructured additive plant perturbations, which directly yield uncertainty frequency weighting function. Second, based on the set of plant models, we setup robust performance control objectives. Third, we make use of the D–K iteration approach for the controller design. Finally, implementing the controller with a digital signal processor, experiments are carried out. With these experimental results, we show robust performance of the designed control system.**

I. INTRODUCTION

Electromagnetic suspension systems can suspend objects without any contact. The increasing use of this technology in its various forms makes the research extremely active. The electromagnetic suspension technology has already applied to magnetically levitated vehicles, magnetic bearings, and so on. Recent advances on this field are shown in [1], and [5].

Feedback control is indispensable for magnetic suspension systems, since they are essentially unstable systems. To synthesis a feedback control system, a precise mathematical model for the plant is required. It is known, however, that a design model can not always express the behavior of the real physical plant. An ideal mathematical model has various uncertainties such as parameter identification errors, unmodeled dynamics, and neglected nonlinearities. The controller is required to have robustness for stability and performance against uncertainties on the model.

Recently, μ-synthesis , which is constructed with both H_∞ synthesis and μ-analysis, has been developed for the design of robust control systems [7], [8]. Beyond the singular value specifications, the μ-synthesis technique can put both robust stability and robust performance problems in a unified framework. Applications of the μ-synthesis method have been reported in [3]–[4], and [9]. This electromagnetic suspension system is a simple SISO system, but in [3] and [10], the authors also applied the H_∞/μ synthesis to a magnetic bearing, and the effectiveness of this design method was evaluated for a MIMO system. In the case of applications of H_∞/μ control to real physical systems, it is quite important to select appropriate design parameters. These parameters construct some parts of the generalized plant, e.g., uncertainty and performance weightings.

In this paper, we will evaluate μ-synthesis methodology experimentally with a real electromagnetic suspension system. We will model the additive uncertainties and decide the frequency weighting function for uncertainty accurately and reasonably. We will show that the closed-loop system with a μ controller achieves robust performance experimentally.

Manuscript received July 2, 1993; revised May 30, 1994.

M. Fujita is with the School of Information Science, Japan Advanced Institute of Science and Technology, Hokuriku Tatsunokuchi, Ishikawa 923-12, Japan.

T. Namerikawa and F. Matsumura are with the Department of Electrical and Computer Engineering, Kanazawa University 2-40-20 Kodatsuno, Kanazawa 920, Japan.

K. Uchida is with the Department of Electrical Engineering, Waseda University 3-4-1 Okubo, Shinjuku, Tokyo 169, Japan.

IEEE Log Number 9407229.

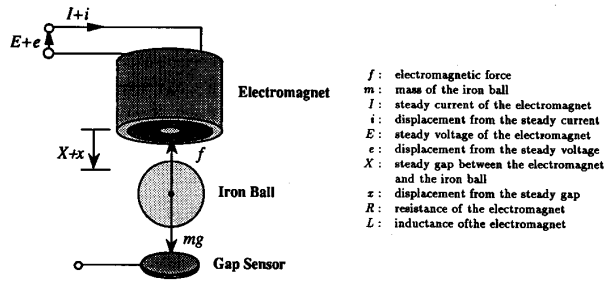

Fig. 1. Schematic diagram of the electromagnetic suspension system.

II. Experimental Setup

A. Electromagnetic Suspension System

The structure of the electromagnetic suspension system is shown schematically in Fig. 1. The objective of our control experiments is to suspend an iron ball stably and firmly without any contact by controlling the attractive forces of an electromagnet. Note that this system is essentially unstable.

In Fig. 1, a cylindrical electromagnet as an actuator is located at the upper part of the experimental system. Mass of the iron ball is 1.75 kg, and it has a diameter of 77 mm. A gap sensor of our own producing is placed at the bottom of the system to measure the gap length between the iron ball and the electromagnet. The sensor is scaled for a gap of 2.4 mm per volt. It is a standard induction probe of eddy-current type. Physical parameters of this experimental machine are shown in Table I.

B. Digital Controller

The experimental machine is controlled by a digital controller using a DSP (digital signal processor). The experimental setup basically consists of the DSP which is sandwiched between A/D and D/A converters. Real-time control is implemented with a processor NEC μPD77230, which can execute one instruction in 150 ns with 32-bit floating point arithmetic. This device has enough fast processing speed to stabilize a relatively simple magnetic suspension system in Fig. 1. The control algorithm is written in the assembly language for the DSP and a software development is assisted by a host personal computer NEC PC-9801 under the MS-DOS environment. The data acquisition board MSP-77230 consists of a 12-bit A/D converter and a 12-bit D/A converter with the maximum conversion speed of 10.5 μs and 1.5 μs, respectively.

The sensor outputs are filtered through an analog low-pass circuit and then converted to digital signals by A/D converters. The DSP calculates the control input signals. These digital signals are converted to analog signals by D/A converters with a range of ± 5 V. The converted signals and the steady current signals are added and amplified by 10 times to actuate the electromagnet. Steady-state voltage of the electromagnet is 24.6 V, and the maximum voltage of a regulated DC power supply is 70.0 V.

III. Model of Electromagnetic Suspension System

Our purpose in this section is to introduce an ideal mathematical model and an uncertainty weighting function for the system. See [4] for details.

TABLE I
Parameters of Electromagnetic Suspension System

Parameter	Maximum Value	Nominal Value	Minimum Value
m [kg]	- - -	1.75	- - -
X [m]	5.50×10^{-3}	5.00×10^{-3}	4.50×10^{-3}
I [A]	1.18	1.06	0.93
x [m]	5.00×10^{-4}	0	-5.00×10^{-4}
i [A]	1.18×10^{-1}	0	-1.26×10^{-1}
L [H]	5.57×10^{-1}	5.08×10^{-1}	4.65×10^{-1}
R [Ω]	$2.37 \times 10^{+1}$	$2.32 \times 10^{+1}$	$2.27 \times 10^{+1}$
k [Nm^2/A^2]	3.35×10^{-4}	2.90×10^{-4}	2.53×10^{-4}
x_0 [m]	-3.32×10^{-4}	-6.41×10^{-4}	-9.42×10^{-4}
Q [Hm]	6.70×10^{-4}	5.79×10^{-4}	5.06×10^{-4}
X_∞ [m]	-3.32×10^{-4}	-6.41×10^{-4}	-9.42×10^{-4}
L_0 [H]	3.96×10^{-1}	3.75×10^{-1}	3.54×10^{-1}

A. Model Structures

We will employ four different model structures for the system depicted in Fig. 1. All of the models are finite-dimensional, linear, and time-invariant of the following state-space form

$$\dot{x} = Ax + Bu, \qquad y = Cx$$
$$x = [x \quad \dot{x} \quad i]^T, \qquad u = e, \qquad y = x. \tag{3.1}$$

First, we introduce ideal mathematical models for the real electromagnetic suspension system. Due to the idealizing assumptions that we make, two types of ideal mathematical models can be derived hereafter, which are composed of nonlinear differential equations. We define them as Type[A] and Type[B], respectively.

Since the behavior of the electromagnetic force is nonlinear, we then employ the linearization procedure around an operating point. To account for the neglected nonlinearity, we derive two types of linear model, respectively. Thus, we will derive four linear models according to the following manners:

- *Model[A1]:* L = CONSTANT; and the nonlinearity of the electromagnetic forces are approximated up to the first-order term in the Taylor series expansion.
- *Model[A2]:* L = CONSTANT; and the nonlinearity of the electromagnetic forces are approximated up to the second-order term in the Taylor series expansion.
- *Model[B1]:* $L = L(x)$; and the nonlinearity of the electromagnetic forces are approximated up to the first-order term in the Taylor series expansion.
- *Model[B2]:* $L = L(x)$; and the nonlinearity of the electromagnetic forces are approximated up to the second-order term in the Taylor series expansion.

1) Ideal Mathematical Model—Type[A]: We will derive ideal mathematical models for the real electromagnetic suspension system, where the following assumptions on the electromagnet are considered.

- A.1) Magnetic permeability of the electromagnet is infinity.
- A.2) Magnetic flux density and magnetic field have not hysteresis, and they are not saturated.
- A.3) Eddy current in the magnetic pole can be neglected.

Using A.1) and A.2), we can treat the coil inductance L as a function of variable x. Then, the system can be written by the following nonlinear differential equations

$$m\frac{d^2x}{dt^2} = mg - f, \qquad f = k\left(\frac{i}{x+x_0}\right)^2,$$
$$e = Ri = \frac{d}{dt}\{L(x)i\} \tag{3.2}$$

where the coefficients k and x_0 in (3.2) are constants determined by identification experiments. Further, we introduce another assumption for Type[A].

- A.A) The coil inductance is constant near an operating point. Furthermore, the electromotive forces due to the differential of gap can be neglected.

Then from (3.2), we get

$$e = Ri + L_c\frac{di}{dt}. \tag{3.3}$$

The ideal mathematical model: Type[A] is represented by (3.2) and (3.3).

Model[A1]: In view of (3.2) and (3.3), we can obtain the linear model (3.4)

$$A = \begin{bmatrix} 0 & 1 & 0 \\ \dfrac{2kI^2}{m(X+x_0)^3} & 0 & -\dfrac{2kI}{m(X+x_0)^2} \\ 0 & 0 & -\dfrac{R}{L} \end{bmatrix},$$
$$B = \begin{bmatrix} 0 \\ 0 \\ \dfrac{1}{L} \end{bmatrix}, \qquad C = \begin{bmatrix} 1 \\ 0 \\ 0 \end{bmatrix}^T. \tag{3.4}$$

Model[A2]: We can further obtain another linear model (3.5)

$$A = \begin{bmatrix} 0 & 1 & 0 \\ \dfrac{2kI^2}{m(X+x_0)^3}\Delta y & 0 & -\dfrac{2kI}{m(X+x_0)^2}\Delta y \\ 0 & 0 & -\dfrac{R}{L} \end{bmatrix},$$
$$B = \begin{bmatrix} 0 \\ 0 \\ \dfrac{1}{L} \end{bmatrix}, \qquad C = \begin{bmatrix} 1 \\ 0 \\ 0 \end{bmatrix}^T,$$
$$\Delta x = \frac{x}{X+x_0}, \qquad \Delta i = \frac{i}{I},$$
$$\Delta y = 1 - \frac{3}{2}\Delta x + \frac{1}{2}\Delta i. \tag{3.5}$$

In this way, we deal with the deviation x and i as fixed numbers, at the second-order term in the Taylor series expansion and include them in the matrix A as Δx, Δi and Δy.

2) Ideal Mathematical Model—Type[B]: For the ideal mathematical model Type[B], we also consider the assumptions A.1), A.2), A.3) and here in addition to them, we introduce the next assumption A.B) instead of A.A). Using this assumption, we can obtain more accurate model than one of Type[A].

- A.B) The coil inductance L is a function of a gap x, and written as follows

$$L(x) = \frac{Q}{x + X_\infty} = L_0 \tag{3.6}$$

where the coefficients Q, X_∞ and L_0 are also the constants determined by identification experiments. For any given current i in a coil with inductance L, the magnetic co-energy is shown as $\frac{1}{2}Li^2$. Hence electromagnetic forces between the electromagnet and the iron ball in (3.2) is equal to the change rate of co-energy with respect to the distance x, i.e.,

$$f = \frac{\partial}{\partial x}\left\{\frac{1}{2}L(x)i^2\right\} = \frac{1}{2}i^2\frac{\partial L(x)}{\partial x}$$
$$= \frac{Q}{2}\left(\frac{i}{x+X_\infty}\right)^2. \tag{3.7}$$

Comparing (3.2) with (3.7)

$$X_\infty = x_0, \qquad Q = 2k. \tag{3.8}$$

Then from (3.2), (3.6) and (3.8), we get

$$e = Ri - \frac{2ki}{(x+x_0)^2}\frac{dx}{dt} + \left(\frac{2k}{x+x_0} + L_0\right)\frac{di}{dt}. \tag{3.9}$$

Now we obtained the ideal mathematical model: Type[B] which is constructed with (3.2) and (3.9).

Model[B1]: From (3.2) and (3.9), the linear model (3.10) (as shown at the bottom of the page) is derived.

Model[B2] Moreover, the linear model (3.11) can be derived, as shown at the bottom of the page.

Thus, now we obtained four linear model structures: Model[A1], Model[A2], Model[B1], and Model[B2].

$$A = \begin{bmatrix} 0 & 1 & 0 \\ \dfrac{2kI^2}{m(X+x_0)^3} & 0 & -\dfrac{2kI}{m(X+x_0)^2} \\ 0 & \dfrac{2kI}{(X+x_0)\{2k+L_0(X+x_0)\}} & -\dfrac{R(X+x_0)}{2k+L_0(X+x_0)} \end{bmatrix},$$
$$B = \begin{bmatrix} 0 \\ 0 \\ \dfrac{X+x_0}{2k+L_0(X+x_0)} \end{bmatrix}, \qquad C = \begin{bmatrix} 1 \\ 0 \\ 0 \end{bmatrix}^T. \tag{3.10}$$

$$A = \begin{bmatrix} 0 & 1 & 0 \\ \dfrac{2kI^2}{m(X+x_0)^3}\Delta y & 0 & -\dfrac{2kI}{m(X+x_0)^2}\Delta y \\ 0 & \dfrac{2kI(1-2\Delta x+\Delta i)}{(X+x_0)\{2k(1-\Delta x)+L_0(X+x_0)\}} & -\dfrac{R(X+x_0)}{2k(1-\Delta x)+L_0(X+x_0)} \end{bmatrix},$$
$$B = \begin{bmatrix} 0 \\ 0 \\ \dfrac{X+x_0}{L_0(X+x_0)+2k(1-\Delta x)} \end{bmatrix}, \qquad C = \begin{bmatrix} 1 \\ 0 \\ 0 \end{bmatrix}^T. \tag{3.11}$$

TABLE II
PERTURBED MODELS

Perturbed Model	Model Structure	Parameter Change
model(1a)	Model[A1]	$k \rightarrow k\_max$
model(1b)	Model[A1]	$k \rightarrow k\_min$
model(2a)	Model[A1]	$x_0 \rightarrow x_0\_max$
model(2b)	Model[A1]	$x_0 \rightarrow x_0\_min$
model(3a)	Model[A1]	$R \rightarrow R\_max$
model(3b)	Model[A1]	$R \rightarrow R\_min$
model(4a)	Model[A1]	$L \rightarrow L\_max$
model(4b)	Model[A1]	$L \rightarrow L\_min$
model(5a)	Model[A2]	$x' \rightarrow x'\_max$
model(5b)	Model[A2]	$x' \rightarrow x'\_min$
model(6a)	Model[A2]	$i' \rightarrow i'\_max$
model(6b)	Model[A2]	$i' \rightarrow i'\_min$
model(7a)	Model[B1]	$k \rightarrow k\_max$
model(7b)	Model[B1]	$k \rightarrow k\_min$
model(8a)	Model[B1]	$x_0 \rightarrow x_0\_max$
model(8b)	Model[B1]	$x_0 \rightarrow x_0\_min$
model(9a)	Model[B1]	$R \rightarrow R\_max$
model(9b)	Model[B1]	$R \rightarrow R\_min$
model(10a)	Model[B1]	$L_0 \rightarrow L_0\_max$
model(10b)	Model[B1]	$L_0 \rightarrow L_0\_min$
model(11a)	Model[B2]	$x' \rightarrow x'\_max$
model(11b)	Model[B2]	$x' \rightarrow x'\_min$
model(12a)	Model[B2]	$i' \rightarrow i'\_max$
model(12b)	Model[B2]	$i' \rightarrow i'\_min$

B. Model Parameters

To account for unpredictable perturbations in the model parameters, we will set the nominal value as well as the possible max./min. value of each parameter in every linear model. To obtain the possible max./min. value of each parameter, consider the steady-state gap X = 5.0 mm (nominal). Now let us perturb it with X = 4.5 mm and X = 5.5 mm (perturbed $\pm$0.5 mm). And, for these cases, we measured the three sets of the parameter values. The results of measurements are shown in Table II.

C. Nominal Model

We will form the nominal model using the simplest Model[A1] structure and the nominal model parameter (X= 5.0 mm case). Its state-space form is then of the following form

$$A_{nom} = \begin{bmatrix} 0 & 1 & 0 \\ 4481 & 0 & -18.43 \\ 0 & 0 & -45.69 \end{bmatrix},$$

$$B_{nom} = \begin{bmatrix} 0 \\ 0 \\ 1.969 \end{bmatrix}, \quad C_{nom} = \begin{bmatrix} 1 \\ 0 \\ 0 \end{bmatrix}^T. \tag{3.12}$$

And the corresponding nominal transfer function is

$$G_{nom} = \frac{-36.27}{(s+66.94)(s-66.94)(s+45.69)}. \tag{3.13}$$

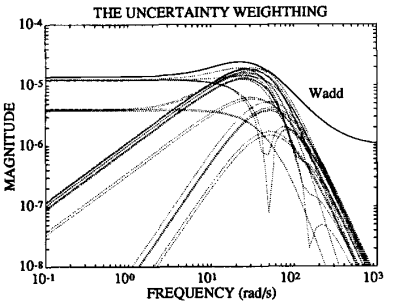

Fig. 2. Uncertainty weighting.

D. Modeling Unstructured Uncertainty

To account for unstructured uncertainties, we should consider not only a nominal model but also a set of plant models in which the real system is assumed to reside. Considering only unstructured uncertainties, we get all unstructured uncertainties together into one-full block uncertainty.

To estimate the quantities of additive model perturbations, we employ differences of gain between the nominal transfer function and the perturbed transfer function with only one parameter changed and the others fixed, where we did not consider that plural parameters change together. In such a way, 24 perturbed models have been employed. They are shown in Table II. With these notations, we can define the corresponding perturbed transfer functions $\hat{G}_{ij}$ in an obvious way

$$\Delta_{ij} := \hat{G}_{ij} - G_{nom} \quad (1 \le i \le 12, j = a, b). \tag{3.14}$$

Frequency responses of these additive perturbations $|\Delta_{ij}(j\omega)|$ are plotted in Fig. 2, with 24 dotted lines. Now let us consider the set of plant models. Here we assume the following form

$$G := \{G_{nom} + \Delta_{add} W_{add} : ||\Delta_{add}||_\infty \le 1\} \tag{3.15}$$

in which the real plant is assumed to reside. All of the uncertainties are captured in the normalized, unknown transfer function Δ_{add}. It is natural to choose the uncertainty weighting W_{add} as follows (shown in Fig. 2). Here it should be noted that the magnitude of the uncertainty weighting W_{add} covers all the model perturbations shown in Fig. 2

$$W_{add} = \frac{1.4 \times 10^{-5}(1+s/8)(1+s/170)(1+s/420)}{(1+s/30)(1+s/35)(1+s/38)}. \tag{3.16}$$

IV. DESIGN

A. Control Objectives

Electromagnetic suspension system is essentially unstable. We must design a robust controller to stabilize the closed-loop system; furthermore, we would like to design a controller to maintain the performance against unpredictable disturbances and the uncertainties.

Let us consider the feedback structure shown in Fig. 3. The box represents the set of the models: $\mathbf{G}$ of the real system. Robust stability requirement for the additive uncertainty can be evaluated using the closed-loop transfer function KS, where $S := (I + GK)^{-1}$. Hence robust stability test for $G \in \mathbf{G}$ is equivalent to

$$||W_{add_r} K(I + G_{nom}K)^{-1} W_{add_l}||_\infty < 1. \tag{4.1}$$

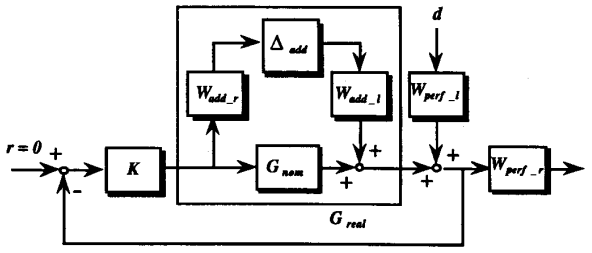

Fig. 3. Feedback structure.

It is noted in Fig. 3 that we factor the uncertainty weighting as $W_{add} = W_{add_l} \times W_{add_r}$, where

$$W_{add_l} = 1.0 \times 10^{-5},$$
$$W_{add_r} = \frac{1.4 \times (1 + s/8)(1 + s/170)(1 + s/420)}{(1 + s/30)(1 = s/35)(1 + s/38)}. \quad (4.2)$$

To reject the disturbances at low frequency band, the performance weighting function W_{perf} is now chosen as

$$W_{perf} = \frac{200.0}{1 + s/0.1}. \quad (4.3)$$

We also factor the performance weighting as $W_{perf} = W_{perf_l} \times W_{perf_r}$, where

$$W_{perf_l} = 1.0 \times 10^{-5}, \quad W_{perf_r} = \frac{2.0 \times 10^7}{1 + s/0.1}. \quad (4.4)$$

In practical situation, however, we would like to achieve this performance specification for all the possible plant $G \in \mathbf{G}$. A necessary and sufficient condition for this robust performance is

$$\|W_{perf_r}(I + GK)^{-1}W_{perf_l}\|_\infty < 1, \quad \forall G \in \mathbf{G}. \quad (4.5)$$

Now the control objective is to find a stabilizing controller K which achieves the following two conditions

- The closed-loop system remains internally stable for every plant model $G \in \mathbf{G}$,
- The weighted sensitivity function satisfies the performance test (4.5) for every plant $G \in \mathbf{G}$.

The design objectives have been specified as the requirements for particular closed loop transfer functions with the frequency weighting functions W_{add} and W_{perf}. The above control objectives exactly fit in the μ-synthesis framework by introducing a fictitious uncertainty block Δ_{perf}. Rearranging the feedback structure in Fig. 3, we can build the interconnection structure shown in Fig. 4.

B. μ-Synthesis

We first define a block structure $\boldsymbol{\Delta}_P$ as

$$\boldsymbol{\Delta}_P := \left\{ \begin{bmatrix} \Delta_{add} & 0 \\ 0 & \Delta_{perf} \end{bmatrix} : \Delta_{add} \in \boldsymbol{C}, \Delta_{perf} \in \boldsymbol{C} \right\}. \quad (4.6)$$

Next, consider a generalized plant P partitioned as

$$P = \begin{bmatrix} P_{11} & P_{12} \\ P_{21} & P_{22} \end{bmatrix}. \quad (4.7)$$

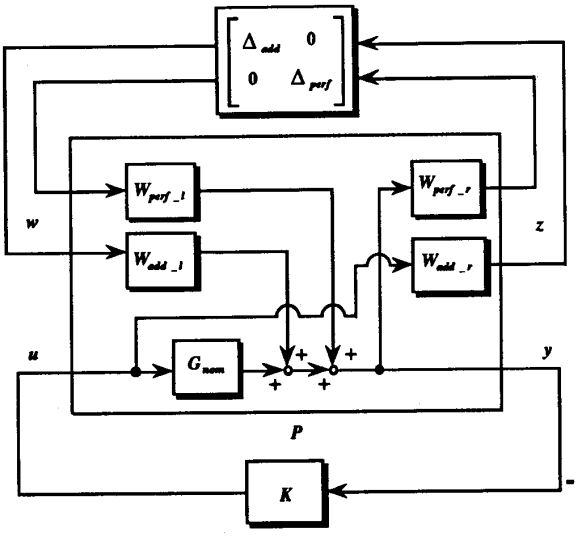

Fig. 4. Interconnection structure.

Obviously in Fig. 4, we can get a lower linear fractional transformation $\mathcal{F}_l(P, K)$ on P by K

$$\mathcal{F}_l(P, K) := P_{11} + P_{12}K(I - P_{22}K)^{-1}P_{21}. \quad (4.8)$$

Finally, robust performance condition is equivalent to the following structured singular value μ test

$$\sup_{\omega \in \mathbf{R}} \mu_{\boldsymbol{\Delta}_P}(\mathcal{F}_l(P, K)(j\omega)) < 1. \quad (4.9)$$

The complex structured singular value $\mu_{\boldsymbol{\Delta}_P}$ is defined as

$$\mu_{\boldsymbol{\Delta}_P}(M) := \frac{1}{\min\{\bar{\sigma}(\Delta : \Delta \in \boldsymbol{\Delta}, \det(I - M\Delta) = 0\}} \quad (4.10)$$

unless no $\Delta \in \boldsymbol{\Delta}$ makes $I - M\Delta$ singular, in which case $\mu_{\boldsymbol{\Delta}}(M) := 0$. In this case a matrix M in (4.10) belongs to $\mathbf{C}^{\mathbf{2\times 2}}$.

C. D-K iteration

Unfortunately, it is not known how to obtain a controller K achieving the structured singular value test (4.9) directly. But we can obtain the lower and upper bounds of μ. Our approach taken here is the so-called D-K iteration procedure.

The D-K iteration involves a sequence of minimizations over either K or D while holding the other fixed, until a satisfactory controller is constructed. First, for $D = I$ fixed, the controller K_1 is synthesized using the well-known state-space H_∞ optimization method. Let $P_1 = P$ denote the given open-loop interconnection structure in Fig. 4, and $\mathcal{F}_l(P, K)$ be the closed-loop transfer function from the disturbances w to the errors z.

Then, solving the following H_∞ control problem

$$\|\mathcal{F}_1(P_1, K_1)\|_\infty < \gamma_1, \quad \gamma_1 = 1.3. \quad (4.11)$$

The problem (4.11) yields the central controller K_1 as shown in (4.12) found at the bottom of the page.

$$K_1 = \frac{-5.22 \times 10^8 (s + 12.46)(s + 30.0)(s + 35.0)(s + 38.0)(s + 45.69)(s + 66.94)}{(s + 0.10)(s + 31.6 - j5.12)(s + 31.6 + j5.12)(s + 39.77)(s + 315.2 - j329.6)(s + 315.2 + j329.6)(s + 734.7)} \quad (4.12)$$

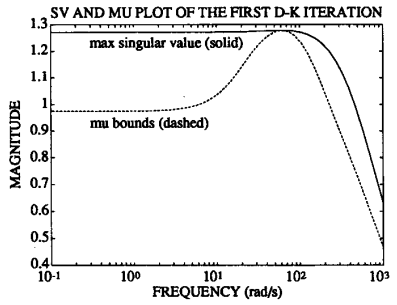

Fig. 5. $\bar{\sigma}$ and μ plot of the first D-K iteration.

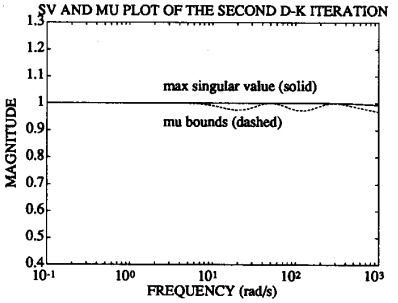

Fig. 6. $\bar{\sigma}$ and μ plot of the second D-K iteration.

Here we try to assess robust performance of this closed-loop system using μ-analysis associated with the block structure (4.6). The maximum singular value and μ upper bound of the closed-loop transfer function $\mathcal{F}_l(P_1, K_1)$ are plotted in Fig. 5. It is noteworthy to point out that the peak value of the upper bound μ plot is not less than one. This reveals that the closed-loop system with this H_∞ controller K_1 does not achieve robust performance condition.

Next, the above calculations of μ produce a scaling matrix at each frequency. In this design, we try to fit the curve using a first-order transfer function.

Now, let P_2 denote the new open-loop interconnection structure absorbing the scaling matrix D. This time, from the following H_∞ control problem

$$||\mathcal{F}_l(P_2, K_2)||_\infty < \gamma_2, \quad \gamma_2 = 1.0 \tag{4.13}$$

we can calculate the controller K_2 as found in (4.14) as shown at the bottom of the page.

The maximum singular value and μ upper bound of this closed-loop system are plotted in Fig. 6. Since the value of μ is less than one in Fig. 6, robust performance condition is now achieved.

V. Experimental Results

The designed controllers K_1 and K_2 are continuous-time systems. To implement these two controllers with the digital controller, we discretized them via the well known Tustin transform. The controllers K_1 and K_2 are discretized at the sampling period of 45μs and 60μs, respectively.

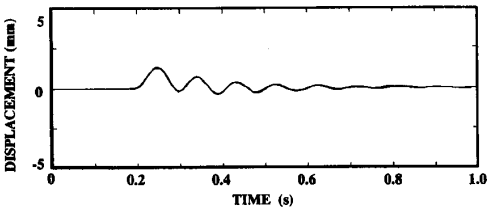

Fig. 7. Response to step disturbance with $\mathbf{K}_1$ (−17.15N).

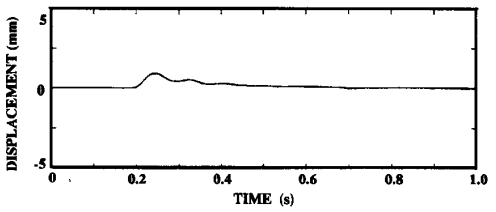

Fig. 8. Response to step disturbance with $\mathbf{K}_2$ (−17.15N).

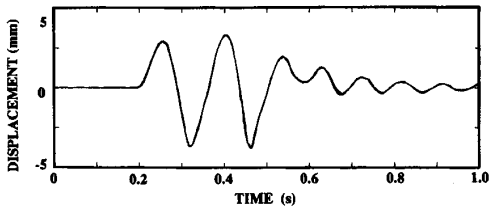

Fig. 9. Response to step disturbance with $\mathbf{K}_1$ (−34.30N).

We succeeded in the stable suspension of the iron ball using both of the controllers K_1 and K_2. In the Section IV, robust stability and robust performance objectives were considered as the control problems. The obtained H_∞ controller K_1 achieves robust stability condition, and μ controller K_2 achieves not only robust stability but also robust performance specification. Hence, we will evaluate robust performance as well as robust stability of the closed-loop systems with responses against various external disturbances.

There the disturbances are added to the experimental system as an applied voltage in the electromagnet. It is noted that there are four types of disturbances. Taking account that the steady-state force of the electromagnet is equal to 17.15 N, we added the following disturbance forces to the floating iron ball

downward 17.15 N, downward 34.30 N.

These disturbances are large enough to evaluate the robustness of both these two controllers. Experimental results are shown in Figs. 7–10.

First of all, these experimental results in Figs. 7–10 show that the iron ball is suspended. Responses in Fig. 9 are vibrating extremely, however, their vibration get on the decrease. This shows the closed-loop systems with both the controllers K_1 and K_2 remain stable against these disturbances. Comparing Fig. 7 with Fig. 9, the responses with K_1 deteriorate extremely against relatively large disturbances. While in Fig. 8 and Fig. 10, the responses with the controller K_2 maintain good transient responses against these disturbances. Now we can see the following observation.

$$K_2 = \frac{-8.01 \times 10^9 (s+10.54)(s+15.75)(s+30.0)(s+35.0)(s+38.0)}{(s+0.10)(s+19.59-j5.32)(s+19.59+j5.32)(s+38.48-j2.70)(s+38.48+j2.70)} \times \frac{(s+45.69)(s+66.94)(s+169.6)}{(s+176.6)(s+420.1-j272.8)(s+420.1+j272.8)(s+8180)}. \tag{4.14}$$

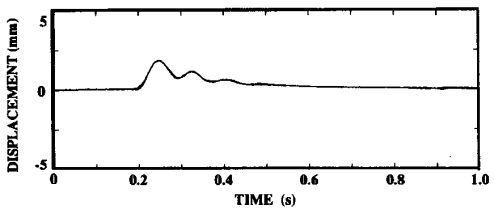

Fig. 10. Response to step disturbance with $\mathbf{K}_2$ (−34.30N).

- The closed-loop system with the μ controller K_2 achieves robust performance, while the closed-loop system with the H_∞controller K_1 does not.

VI. Conclusions

In this paper, we experimentally evaluated a controller designed by μ-synthesis methodology with an electromagnetic suspension system. We have obtained a nominal mathematical model as well as a set of plant models in which the real system is assumed to reside. With this set of the models we designed the control system to achieve robust performance objective utilizing μ-synthesis method.

First, four types of different model structures were derived based on the several idealizing assumptions for the real system. Second, for every model, the nominal value as well as the possible maximum and minimum values of each model parameter was determined by measurements and/or experiments. Third, a nominal model was naturally chosen. This model has the simplest model structure of all four models and makes use of nominal parameter values. Then, model perturbations were defined to account for additive unstructured uncertainties from such as neglected nonlinearities and model parameter errors. Fourth, we defined a family of plant models where the unstructured additive perturbation was employed. The method to model the plant as belonging to a family or set plays a key role for systematic robust control design. Fifth, we setup robust performance objective as a structured singular value test. Next, for the design, the D-K iteration approach was employed. Finally, the experimental results showed that the closed-loop system with the μ-controller achieves not only nominal performance and robust stability, but in addition robust performance.

References

[1] P. Allaire, Ed., "Magnetic bearings," in *Proc. Third Int. Symp. Magnetic Bearings*, Alexandria, VA, 1992.

[2] G. J. Balas, P. Young, and J. C. Doyle, "The process of control design for the NASA Langley minimast structure," in *Proc. Amer. Contr. Conf.*, Boston, MA, 1991, pp. 562–567.

[3] M. Fujita, K. Hatake, F. Matsumura, and K. Uchida "An experimental evaluation and comparison of H_∞/μ control for a magnetic bearing," in *Proc. 12th IFAC World Congress*, Sydney, Australia, 1993, pp. 393–398.

[4] M. Fujita, T. Namerikawa, F. Matsumura, and K. Uchida, "μ-synthesis of an electromagnetic suspension system," in *Proc. 31st IEEE Conf. Decis. Contr.*, Tucson, AZ, 1992, pp. 2574–2579.

[5] T. Higuchi, "Magnetic bearings," in *Proc. Second Int. Symp. Magnetic Bearings*, Tokyo, Japan, 1990.

[6] F. Matsumura and S. Tachimori, "Magnetic suspension system suitable for wide range operation (in Japanese)," *Trans. IEE of Japan*, vol. 99-B, pp. 25–32, 1978.

[7] A. Packard and J. Doyle, "The complex structured singular value," *Automatica*, vol. 29, no. 1, pp. 71–109, 1993.

[8] G. Stein and J. C. Doyle, "Beyond singular values and loop shapes," *J. Guidance*, vol. 14, no. 1, pp. 5–16 1991.

[9] M. Steinbuch, G. Schootstra, and O. H. Bosgra, "Robust control of a compact disc player," in *Proc. IEEE Conf. Decis. Contr.*, Tucson, AZ, 1992, pp. 2596–2600.

[10] M. Fujita, K. Hatake, and F. Matsumura, "Loop shaping based robust control of a magnetic bearing," *IEEE Contr. Syst. Mag.*, vol. 13, no. 4, pp. 57–65, Aug. 1993.

Parameter-Dependent Lyapunov Functions and the Popov Criterion in Robust Analysis and Synthesis

Wassim M. Haddad and Dennis S. Bernstein

***Abstract*— Many practical applications of robust feedback control involve constant real parameter uncertainty, whereas small gain or norm-bounding techniques guarantee robust stability against complex, frequency-dependent uncertainty, thus entailing undue conservatism. Since conventional Lyapunov bounding techniques guarantee stability with respect to time-varying perturbations, they possess a similar drawback. In this paper we develop a framework for parameter-dependent Lyapunov functions, a less conservative refinement of "fixed" Lyapunov functions. An immediate application of this framework is a reinterpretation of the classical Popov criterion as a parameter-dependent Lyapunov function. This result is then used for robust controller synthesis with full-order and reduced-order controllers.**

I. Introduction

The analysis and synthesis of robust feedback controllers entails a fundamental distinction between parametric and nonparametric uncertainty. Parametric uncertainty refers to plant uncertainty that is modeled as constant real parameters, whereas nonparametric uncertainty refers to uncertain transfer function gains modeled as complex frequency-dependent quantities. In the time domain, nonparametric uncertainty is manifested as time-varying uncertain real parameters.

The distinction between parametric and nonparametric uncertainty is critical to the achievable performance of feedback control systems. For example, in the problem of vibration suppression for flexible space structures, if stiffness matrix uncertainty is modeled as nonparametric uncertainty, then perturbations to the damping matrix will inadvertently be allowed. Predictions of stability and performance for given feedback gains will consequently be extremely conservative, thus limiting achievable performance [1]. Alternatively, this problem can be viewed by considering the classical analysis of Hill's equation (e.g., the Mathieu equation) which shows that time-varying parameter variations can destabilize a system even when the parameter variations are confined to a region in which constant variations are nondestabilizing. Consequently, a feedback controller designed for time-varying parameter variations will unnecessarily sacrifice performance when the uncertain real parameters are actually constant.

Manuscript received August 9, 1991; revised July 28, 1992, August 20, 1993, and May 30, 1994. This work was supported in part by Air Force Office of Scientific Research Grant F49620-92-J-0127 and National Science Foundation Grant ECS-9109558.

W. M. Haddad is with School of Aerospace Engineering Georgia Institute of Technology Atlanta, GA 30332-0150 USA.

D. S. Bernstein is with Department of Aerospace Engineering The University of Michigan Ann Arbor, MI 48109-2118 USA.

IEEE Log Number 9407728.